Ceramics for Environmental and Energy Applications II

Edited by
Fatih Dogan
Terry M. Tritt
Tohru Sekino
Yutai Katoh
Aleksander J. Pyzik
Ilias Belharouak
Aldo R. Boccaccini
James Marra

Volume Editor
Hua-Tay Lin

Ceramic Transactions
Volume 246

The American Ceramic Society

WILEY

Ceramics for Environmental and Energy Applications II

Ceramics for Environmental and Energy Applications II

Ceramic Transactions, Volume 246

A Collection of Papers Presented at the
10th Pacific Rim Conference on
Ceramic and Glass Technology
June 2–6, 2013
Coronado, California

Edited by
Fatih Dogan
Terry M. Tritt
Tohru Sekino
Yutai Katoh
Aleksander J. Pyzik
Ilias Belharouak
Aldo R. Boccaccini
James Marra

Volume Editor
Hua-Tay Lin

WILEY

Published by John Wiley & Sons, Inc., Hoboken, New Jersey.
Published simultaneously in Canada.

Library of Congress Cataloging-in-Publication Data is available.

ISBN: 978-1-118-77124-2
ISSN: 1042-1122

Printed in the United States of America.

10 9 8 7 6 5 4 3 2 1

Contents

CERAMICS FOR NEXT GENERATION NUCLEAR ENERGY

ADVANCES IN PHOTOCATALYTIC MATERIALS FOR ENERGY AND ENVIRONMENTAL APPLICATIONS

CERAMICS ENABLING ENVIRONMENTAL PROTECTION: CLEAN AIR AND WATER

Preface

This Ceramic Transactions volume represents 25 selected papers based on presentations in eight symposia during the 10th Pacific Rim Conference on Ceramic and Glass Technology, June 2–6, 2013 in Coronado, California. The symposia include:

- Solid Oxide Fuel Cells and Hydrogen Technology
- Direct Thermal to Electrical Energy Conversion Materials and Applications
- Photovoltaic Materials and Technologies
- Ceramics for Next Generation Nuclear Energy
- Advances in Photocatalytic Materials for Energy and Environmental Applications
- Ceramics Enabling Environmental Protection: Clean Air and Water
- Advanced Materials and Technologies for Electrochemical Energy Storage Systems
- Glasses and Ceramics for Nuclear and Hazardous Waste Treatment

The editors wish to extend their gratitude and appreciation to all the co-organizers for their help and support, to all the authors for their cooperation and contributions, to all the participants and session chairs for their time and efforts, and to all the reviewers for their valuable comments and suggestions. Thanks are due to the staff of the meetings and publication departments of The American Ceramic Society for their invaluable assistance. We also acknowledge the skillful organization and leadership of Dr. Hua-Tay Lin, PACRIM 10 Program Chair.

FATIH DOGAN, Missouri University of Science and Technology, USA
TERRY M. TRITT, Clemson University, USA
TOHRU SEKINO, Tohoku University, Japan
YUTAI KATOH, Oak Ridge National Laboratory, USA
ALEKSANDER J. PYZIK, The Dow Chemical Company, USA
ILIAS BELHAROUAK, Argonne National Laboratory, USA
ALDO R. BOCCACCINI, University of Erlangen-Nuremberg, Germany
JAMES MARRA, Savannah River National Laboratory, USA

RECENT RESEARCH ACTIVITIES FOR FUTURE CHALLENGES IN GLOBAL ENERGY AND ENVIRONMENT IN TOYOTA CENTRAL R&D LABS., INC. (TCRDL)

Tomoyoshi Motohiro[1,2,3]

[1]TOYOTA Central R&D Labs.,Inc.,
41-1, Yokomichi, Nagakute, Aichi, 480-1192, Japan

[2]Graduate School of Engineering, TOYOTA Technological Institute,
2-12-1, Hisakata, Tenpaku-ku, Nagoya, Aichi, 468-8511,Japan

[3]Green Mobility Collaborative Research Center & Graduate School of Engineering, Nagoya University,
Furo-cho, Chikusa-ku, Nagoya, 464-8603, Japan

ABSTRACT

Possible decrease in global supply of conventional oil and greenhouse warming make demands for reduction of oil consumption and diversification of fuels. In association with this, automotive powertrains are also diversifying from conventional internal combustion engine (ICE) into HV, plug-in HV(PHV), EV and fuel-cell HV (FCHV). The main sector is being replaced by HV and PHV, but still stands on ICE. In these hybridized ICE systems, unconventional oils, gaseous-, synthetic- and bio-fuels will be inevitably used more besides conventional fuels. EV as a subsidiary sector for short range use imposes additional demands of electricity from new energy sources. FCHV as another subsidiary sector for route bus and large trucks requests new infrastructures for hydrogen from new energy sources besides industrial by-products. Facing to this situation, it has become important for us to obtain concrete experiences on technologies for future energy sources by conducting R&D by ourselves although the production of energy is out of our business category. R&D for bio-ethanol production from cellulose has been already conducted. This paper describes our other typical recent R&D activities on future energy sources including laser nuclear fusion, solar-pumped lasers, solar cells and artificial photosynthesis, with special attentions to ceramics as key materials.

INTRODUCTION

Possible decrease in global supply of conventional oil and greenhouse warming caused by CO_2 emission make demands for reduction of oil consumption and diversification of fuels. In association with this, automotive powertrains are also diversifying from conventional internal combustion engine (ICE) into hybrid vehicles(HV), plug-in hybrid vehicles(PHV), electric vehicles (EV) and fuel-cell hybrid vehicles (FCHV). The main sector of automobiles is being replaced by HV and PHV, but still stands on ICE. For these hybridized ICE systems, unconventional oils, gaseous fuels, synthetic fuels and bio-fuels will be inevitably used more in addition to the conventional fuels. EV as a subsidiary sector for short range use in imposes

additional demands of electricity which must be supplied from new energy sources as well as conventional power plants. FCHV as an another subsidiary sector for route bus and large trucks requests new infrastructures for hydrogen from new energy sources as well as from industrial by-products.

Facing to this situation, it has become important for us to obtain concrete knowledge and experiences on technologies for future energy sources by conducting R&D by ourselves although the production of energy is out of our business category. R&D for bio-ethanol production from cellulose has been conducted in TCRDL. This paper describes our other typical recent research activities on future energy sources including laser nuclear fusion, solar-pumped lasers, solar cells and artificial photosynthesis, with special attentions to ceramics as key materials.

COMPACT AND HIGH REPETITION(10HZ) LASER NUCLEAR FUSION

It is believed that nuclear fusion can meet the global energy demand with much less burdens on the environment than other energy sources as well as solar energy. However it is still at an immature stage with a lot of technical challenges remaining to be solved. These are being tackled by big science projects such as ITER(International Thermonuclear Experimental Reactor) Project for plasma fusion power plants and LIFE(Laser Inertial Fusion Energy) project in National Ignition Facility in US for inertial fusion power plants. Under an idea that we may achieve laser fusion power plants in a different approach using only two counter laser beams with additional one beam for fast-ignition in contrast to the NIF's 192 laser beams from all directions, a compact and high repetition(10Hz) laser nuclear fusion project has been started by The Graduate School for the Creation of New Photonic Industries, Hamamatsu Photonics K.K., TOYOTA Motor Corporation and TCRDL. We have already observed reasonable amount of neutron yield from D-D fusion by implosion of double-deuterated polystyrene foils separated by 100 μ m by counter- illumination succeeded by fast heating[1]. Figure 1 shows our present status and future plan displayed as neutron yield versus laser energy. Since it is necessary to develop high- repetition MJ lasers before achieving cost and energy pay- back condition as a power plant beyond the break even condition, some intermediate outputs as neutron sources for analysis, medical and industrial applications are envisaged[2]. At present, Nd- doped phosphate laser glass is a key laser medium whether it is NIF's flashlamp- pumped type or our diode-pumped type[3]. It is said that the efficiency can be improved by employing diode- pumped Yb-doped fluorapatite crystals. Moreover, the laser medium may be further scaled up for higher

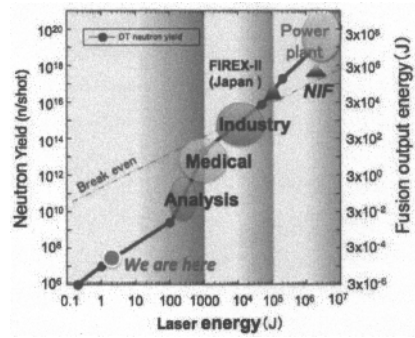

Fig.1. Present status and future plan displayed as neutron yield versus laser energy.

energy output by employing transparent fluorapatite polycrystalline ceramics rather than crystals if micro-domain-control is successful[4,5].

COMPACT SOLAR-PUMPED LASER

High-grade Nd-doped YAG ceramics for laser medium accelerated R&D on solar pumped lasers[6]. Solar pumped lasers usually employ Fresnel lenses or concave mirrors of several meters in diameter to concentrate sunlight into a water-cooled Nd-doped YAG rod of typically 10 mm in diameter and 100mm in length[7]. In contrast, employing an off-axis parabolic mirror of 50mm in diameter and a Nd -doped YAG prismatic rod of 1 x 1 x 5mm in size without water-cooling, we have developed a much more compact solar-pumped laser which can stably emit 1064nm laser light tracking the sun on a commercially available equatorial mounting for amateur astronomers as shown in Fig.2[8]. In the same system, Nd-doped ZBLAN (ZrF_4, BaF_2, LaF_3, AlF_3, NaF) fiber was also successful in laser emission in place of the prismatic rod[9]. The 1064nm laser light or its higher harmonics such as of 532nm is expected to be easily transmitted long distance, to be concentrated into a fine spot to attain high temperature for production of hydrogen from water, and to be converted into electricity using photovoltaic cells with its optical band gap just below the photon energy of the laser light so as to minimize thermal loss.

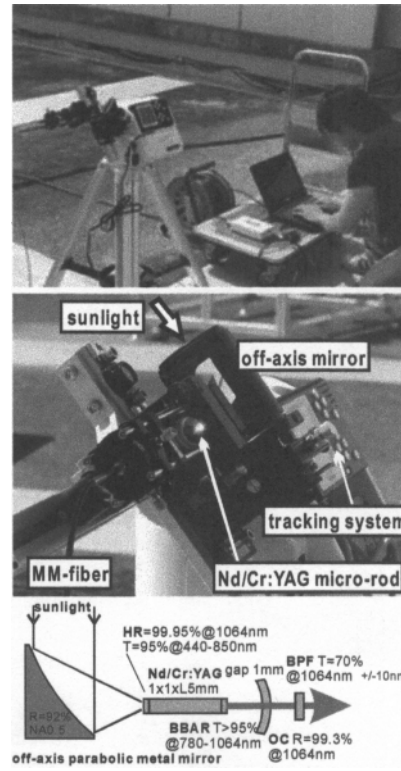

Fig.2 Fabricated compact solar pumped laser mounted on a solar tracker which enables several hours of continuous laser oscillation by tracking the sun.

SOLAR CELLS

Dye-sensitized Solar Cells

R&D on dye-sensitized solar cells(DSSC) comprises of sciences and technologies of ceramics for the optical electrodes typically of sintered nano-porous TiO_2 layers in anatase phase, organic and metal-organic chemistry for sensitizers typically of Ru-complexes and photo-electrochemistry. Conventional solar cell manufacturers working typically on Si p/n junction solar cells have been rather not familiar with such versatile fields but automotive manufacturers

are. Taking this advantage, we have been working on DSSC for more than 15 yeaisplayrs with Aisin Seiki Co. Ltd[10,11]. Figure 3 shows outdoor performance test of battery-operated night-lights charged by dye-sensitized solar cells during daylight near the TOYOTA beam line at the synchrotron orbital radiation site "SPring-8" in Japan. Although the top efficiency over 12% has been reported but there remain still tough challenges of outdoor durability mainly because of degradation of organic dyes and liquid electrolytes[12-14]. Although more than 15 years durability was confirmed for small cells, large modules still have different challenges to be durable. In 2012, there came up possible game-changing technologies reported from plural research groups[15,16] in which sensitizers and electrolyte can be replaced by inorganic materials opening the door to all-solid inorganic dye-sensitized solar cells.

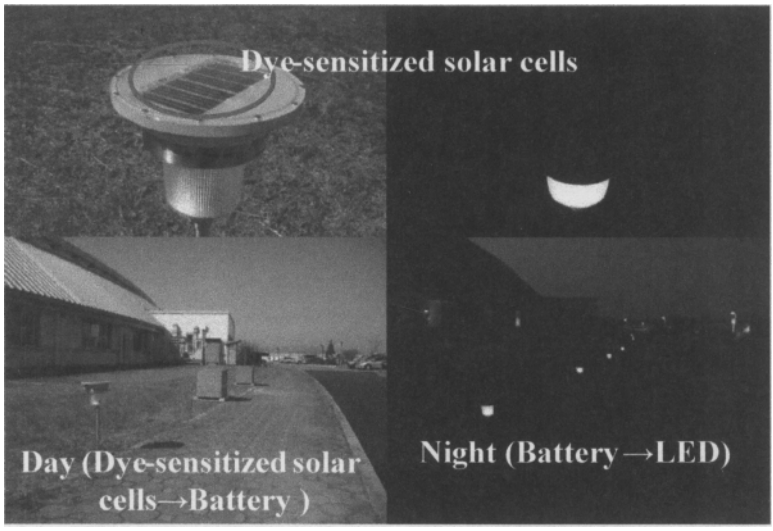

Fig.3 Outdoor performance test of battery-operated LED night-lights charged by monolithic dye-sensitized solar cells in day time (since April, 2009).

Cu_2ZnSnS_4 Thin Film Solar Cells

Inorganic semiconductor solar cells have evolved starting from single-elemental Si, through binary GaAs and CdTe to essentially ternary $Cu(In_{1-x}Ga_x)Se_2$. We have been working on quaternary Cu_2ZnSnS_4 system of kesterite crystal structure since 2006[17-22], because (1) Cu_2ZnSnS_4 is composed of earth-abundant and nontoxic elements, (2) thin-film technologies can reduce both the material cost and the fabrication cost, and (3) the bandgap energy of Cu_2ZnSnS_4 about 1.4eV is optimal for single-junction solar cells leading to the detailed balance limiting efficiency of about 31%[23]. In reactive sintering process, a precursor layer formed on a Mo-coated glass substrate changes into a polycrystalline Cu_2ZnSnS_4 thin film where grain

boundaries take important effect on photovoltaic properties. Although this quaternary system can cause difficulties in stable production, the number of R&D reports is increasing rapidly now as shown in Fig.4 since it uses neither rare elements nor environmental pollutants, and since there is an estimation that only this system can make the electricity generation cost lower than that of Si solar cells. More recently, solution-processed kesterite with an additional element of Se has been successful attaining an energy conversion efficiency beyond 11%[24,25]. On the other hand, a quaternary system without Zn but with Ge: $Cu_2Sn_{0.83}Ge_{0.17}S_3$ was found to have a bandgap of 1.0eV and attained energy conversion efficiency of 6%[26]. This also shows a possibility of higher efficiency constructing a multi-junction type solar cell using this $Cu_2Sn_{0.83}Ge_{0.17}S_3$ for a bottom cell[26].

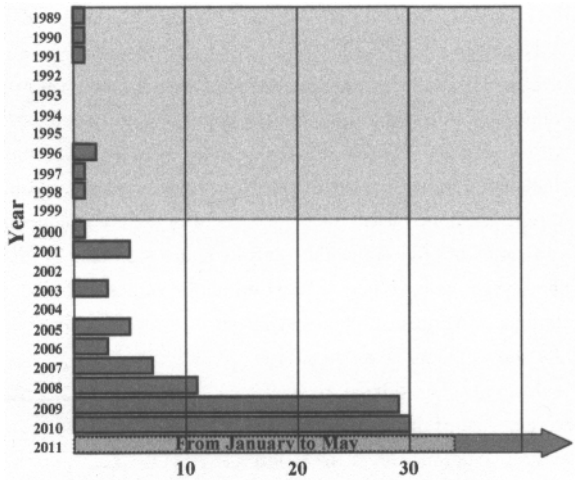

Fig.4 Number of published papers on the topics related to Cu_2ZnSnS_4

The Third Generation Solar Cells

The best strategy to decrease thermal loss of photon energy larger than the bandgap and transmission loss of photon energy less than the bandgap in such a widespread solar spectrum is to construct multi-junction solar cells comprising of plural active materials of different optical absorption edges. To compensate the increase in the fabrication cost to form multi-junction structures, concentration of solar-light onto a solar cell of small area is usually employed. However, since more than half of the sky is shadowed by cloud in average and the percentage of direct sunlight which can be concentrated is lower than 80% even in a typical clear day because of moisture in Japan, the area in which the combination of the solar concentrator and the multi-junction solar cells of small area is applied advantageously is quite limited. The third generation solar cells such as (1) hot-carrier type, (2) multi-exciton generation type, and (3) intermediate-band type have been proposed to decrease the loss mentioned above without using solar concentrators. We have also studied these solar cells both theoretically[27-32] and experimentally [33,34]. Spontaneous formation and arrangement of quantum dots is a key factor in these solar cells. At the present time of writing, however, we are not successful to get any promising perspective for these third generation solar cells.

ARTIFICIAL PHOTOSYNTHESIS OF FORMIC ACID FROM CO_2 AND H_2O ONLY USING SUNLIGHT

Hydrogen production by photo-electrochemical water splitting has been extensively studied all over the world. Hydrogen can be also produced from water electrolysis combined with solar cells. In this situation, syntheses of hydrocarbons using solar energy are much more challenging rather than hydrogen. We had an experience of R&D on visible-light photo-catalysis in nitrogen-doped TiO_2 for photolysis of organic contaminants which has been commercialized as a series of environmental catalysts under the name of VCAT[35]. Based on this experience of photolysis, we have begun R&D on photosynthesis of methanol from CO_2 and H_2O only using sunlight. At present, photo- synthesis of formic acid has been attained[36,37]. Figure 5 schematically shows the process. Here, H_2O molecules are oxidized to yield oxygen using holes formed by photo-excitation in the left electrode and residual electrons are transmitted via conducting wire to the right electrode and reduce CO_2 to form formic acid. To increase selectivity of CO_2 reduction in comparison with hydrogen formation, a Ru-complex layer was formed on the surface of the right electrode. By choosing an appropriate materials combination of the two electrodes, solar-energy conversion efficiency of 0.04% was attained which is 20% of solar-energy conversion efficiency of natural photosynthesis in switchgrass. This was the first achievement of complete artificial photosynthesis from CO_2 and H_2O only using sunlight without applying any bias voltage or additional chemicals in the water. We are continuing effort on further improvement of conversion efficiency and development of electrode materials of lower cost[38].

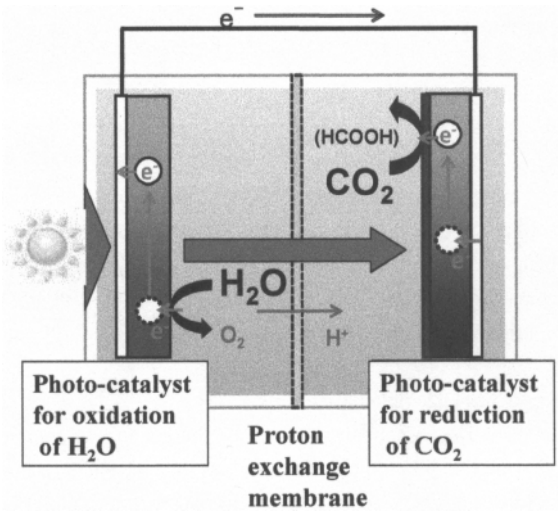

Fig.5 Schematic diagram of artificial photosynhesis of formic acid from CO_2 and H_2O only using sunlight.

SUMMARY

Typical recent research activities on future energy sources including laser nuclear fusion, solar-pumped lasers, solar cells and artificial photosynthesis in TCRDL are reviewed with special attentions to ceramics as key materials. Although every activity introduced here has

attained some innovative milestones, we also realize that there remains still a long way to go to make it practically useful. On the other hand, social and economical environment of energy demand and supply fluctuate quickly including the Fukushima nuclear disaster and the shale gas revolution. Flexible but durable activities of R&D must be kept going on for long term goals as well as short term ones.

REFERENCES

[1]Y. Kitagawa, Y. Mori, O. Komeda, K. Ishii, R. Hanayama, K. Fujita, S. Okihara, T. Sekine, N. Satoh, T. Kurita, M. Takagi, T. Kawashima, H. Kan, N. Nakamura, T. Kondo, M. Fujine, H. Azuma, T. Motohiro, T. Hioki, Y. Nishimura, A. Sunahara, and Y. Sentoku, Fusion Using Fast Heatng of a Compactly Imploded CD Core, Phys. Rev. Lett., **108**, 155001 (2012).

[2]O.Komeda, Y.Mori, R.Hanayama, S. Okihara, K.Fujita, K.Ishii, Y.Kitagawa, T.Kawashima, N.Satoh, T.Sekine, M.Takagi, H.Kan, N.Nakamura, T.Kondo, M.Fujine, H.Azuma, T.Hioki, M.Kakeno, T.Motohiro, Y.Nishimura, Neutron generator using a spherical target irradiated with ultra-intense diode-pumped laser at 1.25 Hz, Fusion Science and Technology **63**, 296-300 (2013).

[3]R. Yasuhara, T. Kawashima, T. Sekine, T. Kurita, T. Ikegawa, O. Matsumoto, M. Miyamoto, H. Kan, H. Yoshida, J. Kawanaka, M. Nakatsuka, N. Miyanaga, Y. Izawa, and T. Kanabe, 213 W average power of 2.4 GW pulsed thermally controlled Nd:glass zigzag slab laser with a stimulated Brillouin scattering mirror, OPTICS LETTERS, **33**, 1711-3 (2008).

[4]J. Akiyama, Y. Sato, and T. Taira, Laser Demonstration of Diode-Pumped Nd^{3+} Doped Fluorapatite Anisotropic Ceramics, Appl. Phys. Express, **4**, 022703 (2011).

[5]J. Akiyama, Y. Sato, and T. Taira, Laser ceramics with rare-earth-doped anisotropic materials, Opt. Lett., **35**, 3598-600 (2010).

[6]J. Lu, K. Ueda, H. Yagi, T. Yanagitani, Y. Akiyama, and A. Kaminskii, Neodymium doped yttrium aluminum garnet($Y_3Al_5O_{12}$) nanocrystalline ceramics — a new generation of solid state laser and optical materials —, J. Alloys and Compounds, **341**, 220-5 (2002).

[7]T.Yabe, T. Ohkubo, S. Uchida, K. Yoshida, M. Nakatsuka, T. Funatsu, A. Mabuti, A. Oyama, K. Kakagawa, T. Oishi, K. Daito, B. Behgol, Y, Nakayama, M. Yoshida, S. Motokoshi, Y. Sato, and C. Baasandash, High-efficiency and economical solar-energy-pumped laser with Fresnel lens and chromium co-doped laser medium, Appl. Phys. Lett., **90**, 261120 (2007).

[8]H.Ito, K. Hasegawa, S. Mizuno, and T. Motohiro, A Solar-pumped Micro-rod Laser without Active Cooling, ALPS2p-20 in Conference Program and Abstracts of The 1st Advanced Lasers and Photon Sources sponsored and organized by The Laser Society of Japan, 26th- 27th, April, 2012 at Pacifico Yokohama, Yokohama, Japan

[9]S. Mizuno, H. Ito, K. Hasegawa, T. Suzuki, and Y. Ohishi, Laser emission from a solar-pumped fiber, Opt. Exp., **20**, 5891-5 (2012).

[10]T. Toyoda, T. Sano, J. Nakajima, S. Doi, S. Fukumoto, A. Ito, T. Tohyama, M. Yoshida, T.

Kanagawa, T. Motohiro, T. Shiga, K. Higuchi, H. Tanaka, Y. Takeda, T. Fukano, N. Katoh, A. Takeichi, K. Takechi, M. Shiozawa, Outdoor performance of large scale DSC Modules, J. Photochem. & Photobiol. A:Chem., **164**, 203-7(2004).

[11]Y. Takeda, N. Kato, K. Higuchi, A. Takeichi, T. Motohiro, S. Fukumoto, T. Sano, and T. Toyoda, Monolithically series-interconnected transparent modules of dye-sensitized solar cells, Sol. Ener. Mater. Sol. Cells, **93**, 808-11(2009)

[12]H. Tanaka, A. Takeichi, K. Higuchi, T. Motohiro, M. Takata, N. Hirota, J. Nakajima, and T. Toyoda, Long-term durability and degradation mechanism of dye-sensitized solar cells sensitized with indoline dyes Sol. Ener. Mater. Sol. Cells, **93**, 1143-8(2009).

[13]N. Kato, Y. Takeda, K. Higuch, A. Takeichi, E. Sudo, H. Tanaka, T. Motohiro, T. Sano, and T. Toyoda, Degradation analysis of dye-sensitized solar cell module after lon g-term stability test under outdoor working condition, Sol. Ener. Mater. Sol. Cells, **93**, 8 93-7(2009).

[14]N. Kato, K. Higuchi, H. Tanaka, J. Nakajima, T. Sano, and T. Toyoda, Improvement in long-term stability of dye-sensitized solar cell for outdoor use, Sol. Ener. Mater. Sol. Cells, **95**, 301-5 (2011) .

[15]I.Chung, B. Lee, J. He, R.P. H. Chang, and M. G. Kanatzidis, All-solid-state dye-sensitized solar cells with high efficiency, nature, **485**, 486-9(2012).

[16]M. M. Lee, J. Teuscher, T. Miyasaka, T. N. Murakami, and H. J, Snaith, Efficient Hybrid Solar Cells Based on Meso-Superstructured Organometal Halide Perovskites, SCIENCE, **338**, 643-7 (2012).

[17]H. Katagiri, K. Jimbo, S. Yamada, T. Kamimura, W. S. Maw, T. Fukano, T. Ito, and T. Motohiro, Enhansed conversion efficiencies of Cu_2ZnSnS_4-based thin film solar cells by using preferential etching technique, Appl. Phys. Express, **1**, 041201 (2008).

[18]J. Paier, R. Asahi, A. Nagoya, and G. Kresse, Cu_2ZnSnS_4 as a potential photovoltaic material: A hybrid Hartree-Fock density functional theory study, Phys. Rev. B, 79, 115126 (2009).

[19]A. Nagoya, and R. Asahi, Defect formation and phase stability of Cu_2ZnSnS_4 photovoltaic material, Phys. Rev. B 81, 113202 (2010).

[20]T. Washio, H. Nozaki, T. Fukano, T. Motohiro, K. Jimbo, and H. Katagiri, Analysis of lattice site occupancy in kesterite structure of Cu_2ZnSnS_4 films using synchrotron radiation x-ray diffraction, J. Appl. Phys., **110**, 074511 (2011).

[21]T. Washio, T. Shinji, S. Tajima, T. Fukano, T. Motohiro, K. Jimbo and H. Katagiri, 6% Efficiency Cu_2ZnSnS_4-based thin film solar cells using oxide precursors by open atmosphere type CVD, J. Mater. Chem., **22**, 4021-4 (2012).

[22]S. Tajima, H. Katagiri, K. Jimbo, N. Sugimoto, and T. Fukano, Temperature Dependence of Cu_2ZnSnS_4 Photovoltaic Cell Properties, Appl. Phys. Express, **5**, 082302 (2012).

[23] W. Shockley, and H. J. Queisser, Detailed Balance Limit of Efficiency of *p-n* Junction Solar Cells, J. Appl. Phys. **32**, 510 (1961).

[24]D. B. Mitzi, O. Gunawan, T. K. Todorov, K. Wang, S. Guha, The path towards a high-performance solution-processed kesterite solar cell, Sol. Ener. Mater. and Sol. Cells, **95**, 1421-36 (2011).

[25] T. K. Todorov, J.Tang, S. Bag, O. Gunawan, T. Gokmen, Y. Zhu, D. B. Mitzi, Beyond 11% Efficiency: Characteristics of State-of-the-Art $Cu_2ZnSn(S,Se)_4$ Solar Cells, Advanced Energy Materials, **3**, 34-8(2013).

[26] M. Umehara, Y. Takeda, T. Motohiro, T. Sakai, H. Awano, and R. Maekawa, $Cu_2Sn_{1-x}Ge_xS_3$ (x =0.17) Thin-Film Solar Cells with High Conversion Efficiency of 6.0%, Appl. Phys. Express, **6**, 045501 (2013).

[27]Y. Takeda, T. Ito, T. Motohiro, D. Konig, S. Shrestha, and G. Conibeer, Hot carrier solar cells operating under practical conditions, J. Appl. Phys.,**105**, 074905 (2009)

[28]Y. Takeda, T. Ito, R. Suzuki, T. Motohiro, S. Shrestha and G. Conibeer, Impact ioniz ation and Auger recombination at high carrier temperature, Sol. Ener. Mater. Sol. Cells **93**, 797-802(2009).

[29]Y.Takeda, T. Motohiro, D. Konig, P. Aliberti, Y. Feng, S. Shrestha, and G. Conibeer, Practical Factors Lowering Conversion Efficiency of Hot Carrier Solar Cells, Appl. Phys. Express, **3**, 104301(2010)

[30]Y. Takeda, and T. Motohiro, Requisites to realize high conversion efficiency of solar cells utilizing carrier multiplication, Sol. Ener. Mater. Sol. Cells., **94**, 1399-405(2010).

[31]Y. Takeda, and T. Motohiro, Intermediate-band-assisted hot-carrier solar cells using indirect-bandgap absorbers, Progress in Photovoltaics: Research and Applications, John Willey & Sons, Ltd.,2012.

[32]Y.Takeda, and T.Motohiro, Hot-Carrier Extraction from intermediate-Band Absorbers through Quantum-Well Energy-Selective Contacts Jpn. J. Appl. Phys.,51, 10ND03_1-6(2012).

[33]K.Nishikawa,Y.Takeda, K.Yamanaka, T.Motohiro, D.Sato,J.Ota, N.Miyashita, Y. Okada, Over 100ns intrinsic radiative recombination lifetime in type II InAs/ GaAs1-xSbx quantum dots J.Appl.Phys.,111, 044325_1-6(2012).

[34]K. Nishikawa, Y. Takeda, T. Motohiro, D. Sato, J. Ota, N. Miyashita, Y. Okada, Extremely long carrier lifetime over 200ns in GaAs wall-inserted type II InAs quantum dots, Applied Physics Letters, **100**, 113105_1-3(2012).

[35]R. Asahi, T. Morikawa, T. Ohwaki, K. Aoki, and Y. Taga, Visible-Light Photocatalysis in Nitrogen-Doped Titanium Oxides, Science, **293**, 269-71 (2001).

[36]S. Sato, T. Morikawa, S. Saeki, T. Kajino and T. Motohiro Visible-Light-Induced Selective CO_2 Reduction Utilizing a Ruthenium Complex Electrocatalyst Linked to a p-Type Nitrogen-Doped Ta_2O_5 Semiconductor, Angew. Chem., Int. Ed., **49**, 5101-5 (2010).

[37]S. Sato, T. Arai, T. Morikawa , K. Uemura , T. M. Suzuki , H. Tanaka , and T. Kajino, Selective CO_2 Conversion to Formate Conjugated with H_2O Oxidation Utilizing Semiconductor/Complex Hybrid Photocatalysts , J. Am. Chem. Soc., **133**, 15240-3 (2011).

[38]T. Morikawa, T. Arai, and T.Motohiro, Photoactivity of p-Type Fe_2O_3 Induced by Anionic/Cationic Codoping of N and Zn, Appl. Phys. Express, **6** , 041201 (2013).

Solid Oxide Fuel Cells and Hydrogen Technology

STRUCTURAL AND ELECTRICAL CHARACTERIZATION OF $Pr_xCe_{0.95-x}Gd_{0.05}O_{2-\delta}$ ($0.15 \leq x \leq 0.40$) AS CATHODE MATERIALS FOR LOW TEMPERATURE SOFC

Rajalekshmi Chockalingam[a], Suddhasatwa Basu[a] *and Ashok Kumar Ganguli[b]
[a]Department of Chemical Engineering, [b]Department of Chemistry Indian Institute of Technology New Delhi, 110016, India

ABSTRACT

Structural and electrical properties $Pr_xCe_{0.95-x}Gd_{0.05}O_{2-\delta}$ ($0.15 \leq x \leq 0.40$) have been investigated as cathode materials for low temperature solid oxide fuel cells. Four compositions of $Pr_xCe_{0.95-x}Gd_{0.05}O_{2-\delta}$(PCGO) have been prepared by varying the Pr content. Phase formation, thermal expansion, ionic conductivity, ionic transference number and electronic conductivity have been studied. XRD results indicate that $Pr_xCe_{0.95-x}Gd_{0.05}O_{2-\delta}$ samples crystallize in the fluorite structure, and no other faces has formed. The coefficient of thermal expansion increases with increasing x, and at x = 0.2 shows CTE value of 13 x 10^{-6} K^{-1} comparable to the CTE value of GDC electrolyte. The ionic transference number decrease while electronic conductivity increase with increasing x. Gd^{3+} contributes to ionic conduction by creating oxygen vacancies and Pr^{4+} contributes electronic conduction by decreasing the band gap of CeO_2. A single cell with configuration $Pr_{0.20}Ce_{0.75}Gd_{0.05}O_{2-\delta}$-$Ce_{0.80}Gd_{0.20}O_{2-\delta}$ (cathode) // $Ce_{0.80}Gd_{0.20}O_{2-\delta}$(electrolyte) // NiO-$Ce_{0.80}Gd_{0.20}O_{2-\delta}$(anode) delivered a maximum power density of 167.9 mW cm^{-2} and current density of 372.5 $mAcm^{-2}$ at 650 °C.

INTRODUCTION

Zirconia based high temperature solid oxide fuel cells (SOFC) suffer due to high cost and lower reliability [1]. Reducing the operating temperature of SOFC below 800 °C is very challenging due to poor catalytic activity of existing cathode materials [2]. Conventional cathode material, $La_{1-x}Sr_xMnO_3$ (LSM) performs poor at low temperatures (500 -650 °C [3]. Several groups have investigated perovskites based materials such as $NdBaCo_{2-x}Cu_xO_{5+\delta}$, $GdBaCo_{1.0}Cu_{1.0}O_{5+\delta}$, $La_{1-x}Sr_xCo_{1-y}FeO_{3-\delta}$ (LSCF), $La_{0.9}Sr_{0.1}Ga_{0.8}Mg_{0.2}O_{3-\delta}$ (LSGM), $Ba_{1-x}Sr_xCo_{1-y}Fe_yO_{3-\delta}$ (BSCF) and $SrCo_{1-y}Sb_yO_{3-\delta}$ (SCS) as alternative cathode materials for intermediate temperature SOFC applications [4-8]. Despite improvements in the area-specific resistance (ASR), these materials do not perform well in the temperature range of 500-650 °C. Recently, Takasu et al.,[8]reported high electronic conductivity for $Ce_{0.60}Pr_{0.40}O_{2-\delta}$ above 600 °C. Nauer et al., [6] studied praseodymia and niobia doped ceria and observed an increase in electrical conductivity with increasing praseodymium content. There were also reports of multi doped ceria to improve the electrical conductivity by lowering the association enthalpy of oxygen vacancies, increase of configuration entropy, modification of elastic strain in the crystal lattice and change in the grain boundary composition [6]. Maffei and Kuriakose [7] doped ceria with gadolinium and praseodymium to reduce the electronic conductivity of ceria and found that double doping scheme is not effective in reducing the electronic conductivity of ceria. Most of the published work till date on Pr and Gd co-doped CeO_2 have focused on its application as an oxygen sensor, or for oxygen storage and oxygen permeability devices and no detailed study has been reported about its suitability as a cathode material for low temperature solid oxide fuel cells. In the present work, structural and electrical properties of the mixed ionic and electronic conducting oxides $Pr_xCe_{0.95-x}Gd_{0.05}O_{2-\delta}$ ($0.15 \leq x \leq 0.40$) have been studied for the application of low temperature SOFC cathode.

EXPERIMENTAL DETAILS

Powders of $Pr_xCe_{0.95-x}Gd_{0.05}O_{2-\delta}$ (PCGO) with x=0.15, 0.20, 0.30 and 0.40 were prepared by conventional solid state route. High purity oxides of CeO_2, Gd_2O_3 and Pr_6O_{11} (99.95%, Alfa Aesar, Johnson Matthey Company, USA) in stoichiometric ratio were ball milled in ethanol for 24 h. The resulting powders were dried at 80 °C for 12 h and pre-calcined at 1100 °C for 6 h. The calcined powders were uni-axially die-pressed at 70 MPa into 13 mm diameter pellets. The samples were vacuum-packed and iso-statically pressed at 250 MPa for 5 minutes. The green pellets were sintered at 1600 °C for 10 h in air with a heating and cooling rate of 2 °C per minute. An X'PERT PRO Panalytical X-ray diffractometer was used to determine the phase and crystal structure of PCGO powder samples. CuKα radiation was generated with an accelerating voltage of 40 kV and current of 30 mA. JCPDS database was used to identify phases. Bulk density of the samples was determined using Archimedes principle using de-ionized water. The microstructures of the sintered samples were evaluated using a scanning electron microscopy (SEM). The thermal expansion measurements were performed in air on the sintered rod shaped specimens with a relative density of > 95% using the NETZSCH 402 PC dilatometer over a temperature range 25-800 °C with a heating rate of 2 °C per min. Standard fused silica sample was used for calibration. Complex impedance measurements were performed in the temperature range, 550-700 °C in air using a AUTOLAB PGSTAT30 FRA in the frequency range from 0.1 Hz to 13 MHz with 10 mV signal amplitude. Nyquist plots were then generated using commercially available nonlinear least square fit software NOVA 1.8 and the conductivity in S/cm was determined for each composition. The ionic transference number has been measured by using a homemade set up. The cell configuration used in our study was pO'_2, Ag //PCGO//Ag, pO''_2. Dried and pure oxygen gas was passed on one side (cathode side) as a reference gas and air or mixture of O_2-Ar gases ranging from 5 to 45% O_2 were passed into the anode side of the cell. The average ionic transference number is calculated using the equation [9]

$$t_0 = \frac{E_O}{E_N} \tag{1}$$

where E_O is the e.m.f. measured under open circuit conditions across the MIEC and E_N is the Nernst potential imposed across the sample. The value of E_N was determined by the activity of electroactive species at the electrode-electrolyte interfaces.

The E_N is given by [9]

$$E_N = \frac{RT}{4F} \ln\left[\frac{pO_2''}{pO_2'}\right] \tag{2}$$

Where, R is the universal gas constant, T is the absolute temperature, F is the Faraday's constant pO_2' and pO_2'' are the partial pressures of oxygen at the two interfaces of the cell.

The total conductivity of PCGO samples were obtained by AC impedance spectroscopy. The ionic conductivity is estimated as

$$\sigma_0 = t_0 \, \sigma_T \tag{3}$$

The electronic conductivityhas been estimated as

$$\sigma_e = (1 - t_0)\,\sigma_T \qquad (4)$$

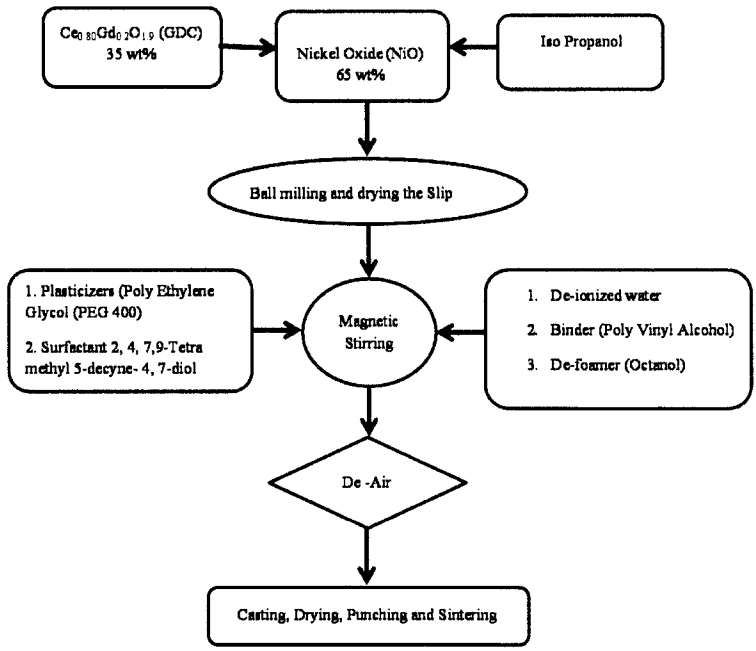

Figure 1. Flow diagram showing various steps involved in the fabrication of NiO-GDC anode tapes via aqueous tape casting.

Figure. 1. shows the flow diagram of various steps involved in the preparation of NiO-GDC anode tapes through an aqueous based tape casting technique [9]. Appropriate amounts of CeO_2 and Gd_2O_3 powders were mixed and ballmilled in ethanol for 24 hours to form a stoichiometric composition of $Ce_{0.8}Gd_{0.2}O_{1.9}$ powder. The resultant powders were dried and calcined at1100 °C for 5 h. The as synthesized $Ce_{0.8}Gd_{0.2}O_{1.9}$ powders were then mixed with NiO powder (99.95%, Alfa Aesar, Johnson Matthey Company, USA) in a weight ratio of 35:65 and again ball milled in isopropanol for 6 h and the slip was dried at 50 °C. The anode materials, NiO-GDC mixture were mixed with deionized water and poly acrylic acid (dispersant) using magnetic stirring for 24 h followed by another 24 h of stirring after adding other ingradients like binder, plasticizer, surfactant etc. The slip was then tape casted and the cast tapes were then allowed to dry over night at room temperature before casting the bilayer of GDC electrolyte. The electrolyte slurry was prepared by mixing appropriate amount of GDC powder, poly vinyl butyral (binder) and menhaden fish oil as dispersant in iso propanol using magnetic stirring for 12 h and the resultant slip was casted on the alreadyprepared anode layer. The thickness of the

anode layer was 1mm and the electrolyte layer was 500 μm. This green anode/electrolyte bilayer was punched into 13 mm diameter disks and cofired at 1500 °C for 10 h hold at heating rate of 1°C per minute. Cathode slurry was prepared by mixing PCGO nano powder and GDC electrolyte powder in a weight ratio 70:30 and appropriate amounts of ethyl cellulose and poly vinyl butyral were added as a pore former and binder respectively and mixed in α-terpineol and made into a fine ink on a magnetic stirrer. This cathode ink was brush painted on the electrolyte side of the sintered anode/electrolyte bilayer, dried and again sintered at 1350 °C for 2h. The sintered single cells consist of 0.5-0.6 mm thick electrolyte layer and 0.3-0.5 mm thick anode and cathode layers respectively. Finally both anode and cathode surfaces were covered with nickel gauze and silver gauze respectively as current collectors, which were then coated with silver conductive ink as a sealant. Silver wires were connected as the connection leads and heat treated at 400 °C for 1 h for a better electrical contact. The as prepared cell was then mounted in between the air and fuel chambers of an indigenously developed stainless steel test station. The cells were tested between 500, 550 and 650 °C with humidified hydrogen gas as the fuel and zero air was used as oxidant. Both gas flow rates were controlled between 40 and 100 mL min^{-1} at 1 atmosphere pressure. The performance analysis of the fuel cells was carried out using Potentistat/Galvanostat (Autolab, PGSTAT 30).

RESULTS AND DISCUSSION

The XRD patterns of $Pr_xCe_{0.95-x}Gd_{0.05}O_{2-\delta}$ ($0.15 \leq x \leq 0.40$) samples sintered at 1600 °C for 10h are shown in Figure. 2. All the samples show fluorite crystal structure and no extra peaks are observed, indicating that no secondary phases are formed. Figure 3 shows the SEM analysis

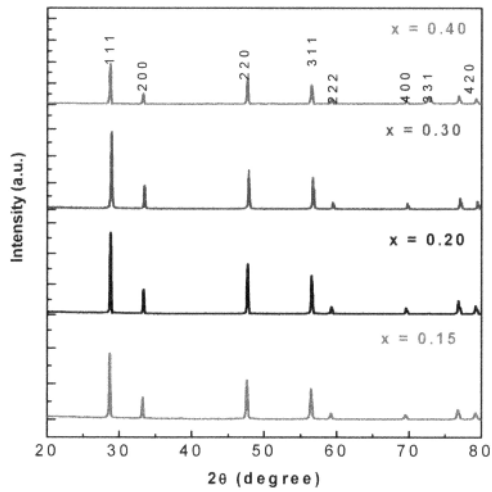

Figure 2.X-ray diffraction analysis of $Pr_{1-x}Ce_xGd_{0.05}O_{2-\delta}$ ($0.15 \leq x \leq 0.40$) cathode samples sintered at 1600 °C for 10 h

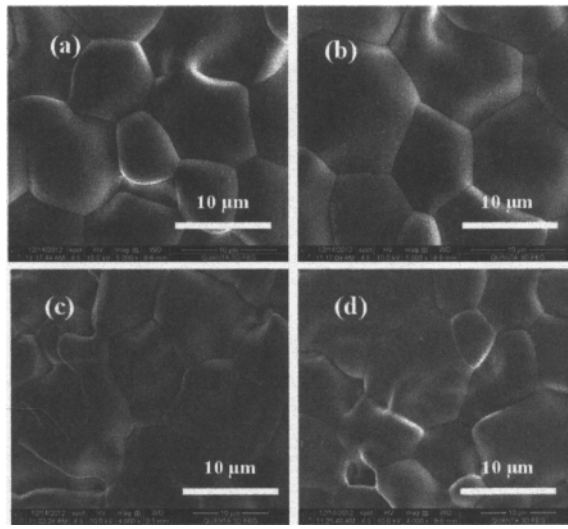

Figure 3.SEM analysis of $Pr_{1-x}Ce_xGd_{0.05}O_{2-\delta}$ ($0.15 \leq x \leq 0.40$) cathode samples (a) x = 0.15 (b) x = 0.20 (c) x = 0.30 and (d) x = 0.40 sintered at 1600 °C for 10 h.

of the fracture surfaces of the cathode samples sintered at 1600 °C for 10h, which indicates well sintered and fully densified samples with a grain size ranging from 5-10 µm size.The density of the samples were estimated by Archemedes principle using deionized water and the percentage density of the samples were shown in figure 4 (a). The percentage density increases with increasing Pr content. The x=0.40 sample exhibited a maximum density of 98% whereas the sample with x =0.15 exhibited 88 %. Figure 4 (b) shows the shrinkage vs Pr content of samples sintered at 1600 °C for 10 h and the shrinkage decreases with increasing Pr content. The results show that sinterability of the sample improved with addition of Pr.

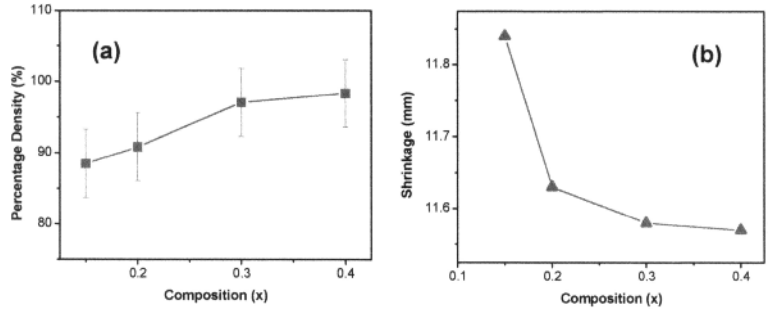

Figure 4. (a) Percentage density and (b) Shrinkage vs composition of $Pr_{1-x}Ce_xGd_{0.05}O_{2-\delta}$ ($0.15 \leq x \leq 0.40$) cathode samples sintered at 1600 °C for 10 h.